Molecular Crystals and Liquid Crystals

Publication details, including instructions for authors and subscription information:
http://www.tandfonline.com/loi/gmcl20

Organic Conductor Based on Nucleobase: Structural and Electronic Properties of a Charge-Transfer Solid Composed of TCNQ Anion Radical and Hemiprotonated Cytosine

Tsuyoshi Murata [a], Kazukuni Nishimura [a] & Gunzi Saito [a]

[a] Division of Chemistry, Graduate School of Science, Kyoto University, Oiwakecho, Kitashirakawa, Sakyo-ku, Kyoto, Japan

Version of record first published: 22 Sep 2010

To cite this article: Tsuyoshi Murata, Kazukuni Nishimura & Gunzi Saito (2007): Organic Conductor Based on Nucleobase: Structural and Electronic Properties of a Charge-Transfer Solid Composed of TCNQ Anion Radical and Hemiprotonated Cytosine, Molecular Crystals and Liquid Crystals, 466:1, 101-112

To link to this article: http://dx.doi.org/10.1080/15421400601150247

Mol. Cryst. Liq. Cryst., Vol. 466, pp. 101–112, 2007

ISSN: 1542-1406 print/1563-5287 online
DOI: 10.1080/15421400601150247

Organic Conductor Based on Nucleobase: Structural and Electronic Properties of a Charge-Transfer Solid Composed of TCNQ Anion Radical and Hemiprotonated Cytosine

Tsuyoshi Murata
Kazukuni Nishimura
Gunzi Saito
Division of Chemistry, Graduate School of Science, Kyoto University, Oiwakecho, Kitashirakawa, Sakyo-ku, Kyoto, Japan

A semiconductive charge-transfer solid was prepared by the reaction of cytosine and TCNQ. Cytosine molecules formed a hemiprotonated cytosine pair by complementary triple hydrogen bonds, and the pairs were then linked by complementary double hydrogen bonds to form infinite ribbons. TCNQ molecules formed uniform segregated columns. The robust hydrogen bonds linking the cytosine and TCNQ molecules preserved the uniform arrangement even at low temperatures. Such structural regulation demonstrated a high conductivity of 3×10^{-2} *S cm*$^{-1}$ *in a fully ionic TCNQ salt by virtue of large transfer interaction and short interplanar distance of TCNQ molecules.*

Keywords: charge-transfer conductor; complementary hydrogen bond; cytosine; Nucleobase; TCNQ

INTRODUCTION

Biomolecular systems have attracted much attention in the recent research on molecule-based materials. Electrical conduction of biomolecules is of particular interest [1]. DNA is one of the candidates for biomolecular conductors, where the one-dimensional (1D) π stack of nucleobases is regarded as a hole transport path [2]. The base pairing of nucleobases by complementary hydrogen bonds (HBs) is an important factor in establishing the DNA duplex. The robust and directional

Address correspondence to Gunzi Saito, Division of Chemistry, Graduate School of Science, Kyoto University, Oiwakecho, Kitashirakawa, Sakyo-ku, Kyoto 606-8502, Japan. E-mail: saito@kuchem.kyoto-u.ac.jp

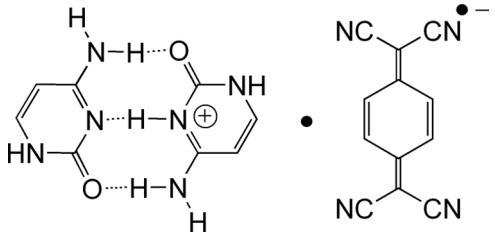

CHART 1 Chemical structure of (**CHC**$^+$)(TCNQ$^{\bullet-}$), 1.

HB features of nucleobases have inspired the exploration of molecular conductors based on the charge-transfer (CT) complexes in tetrathiafulvalene derivatives having nucleobase skeletons [3]. There has been some research into CT solids composed of nucleobases, which provides a deep insight into electrical conduction of DNA. However, no conductive CT solids have been reported [4]. To explore organic conductors incorporating biomolecules, we have investigated the preparation, crystal structure, and electronic properties of the CT solids formed by cytosine (**C**) and TCNQ derivatives [5], and we report here the conductive CT solid composed of a hemiprotonated **C** pair and TCNQ anion radical (TCNQ$^{\bullet-}$) (1, Chart 1).

C is a nucleobase and a Brönsted base (p$K_a = 4.55$) [6], which forms readily protonated cation, **CH**$^+$ in acidic conditions. Furthermore, a pair of **C** and **CH**$^+$, hemiprotonated **C** pair (**CHC**$^+$), where two **C** molecules are connected by complementary triple HBs (Chart 1), have rarely been observed in some salts of **C** [7], its derivatives [8], and established well-defined supramolecular structures such as oligocytidine quadruplex [8b]. The complex formation between **C** and TCNQ, which produced a 2:1 salt of TCNQ$^{\bullet-}$, has been examined by Sheina et al., though no physical and structural studies in the solid state have been elucidated [4c].

EXPERIMENTAL

General Information

Measurements of absorption spectra were done with a KBr disk on a Perkin-Elmer Paragon 1000 series FT-IR (resolution 2 cm^{-1}) for infrared (IR) and near-IR regions (400–7800 cm^{-1}), and on a Shimadzu UV-3100 spectrometer for near-IR, visible, and ultraviolet (UV-vis-NIR) regions (3800–42,000 cm^{-1}). Dc conductivity was measured by a standard two-probe technique by attaching gold wires (15–25 $\mu m\phi$) on samples using gold paste (Tokuriki 8560-1A). Static magnetic

TABLE 1 X-Ray Crystallographic Data of **1** ($C_{20}H_{15}N_{10}O_2$ 427.42 wt) at 200 K and 9 K

Parameter	Value	
	200 K	9 K
Crystal system	triclinic	triclinic
Space group	$P\bar{1}$	$P\bar{1}$
a/Å	3.764(1)	3.724(1)
b/Å	7.408(2)	7.401(4)
c/Å	17.010(5)	16.946(9)
α/°	88.25(2)	88.25(3)
β/°	89.74(2)	89.04(3)
γ/°	84.65(2)	84.71(3)
V/Å^3	472.0(2)	464.8(4)
Z	1	1
d_{calc}/g·cm^{-1}	1.504	1.527
No. of intensity meas.	1801	1725
No. of refined parameters	177	174
R ($F > 4\sigma(F)$)	0.067	0.065
${}_wR_2$	0.198	0.181
GOF	1.032	0.963

susceptibility measurement was done using a Squid magnetosusceptometer (Quantum Design MPMS) from 300 K to 2.0 K.

The intensity data of structural analyses were collected using an oscillator type X-ray imaging plate (DIP-2020K) with a monochromated MoK_α radiation at 200 and 9 K. The structures were solved by direct methods using SHELXS-97 [9]. Refinements of structures were done by the full-matrix least-squares method (SHELXL-97) [9]. Positions of hydrogen atoms were determined by D-synthesis. Parameters were refined by adopting anisotropic and isotropic temperature factors for nonhydrogen and hydrogen atoms, respectively. Selected crystal data and data collection parameters are shown in Table 1. The data was deposited in the Cambridge Crystallographic Data Centre (CCDC 602000 and 602001).

RESULTS AND DISCUSSION

Preparation and Optical Properties

Slow diffusion of **C** and TCNQ in a methanol (MeOH)–acetonitrile (MeCN) mixed solvent at room temperature (RT) produced black plates of **1**. Mixing hot solutions of **C**/MeOH and TCNQ/MeCN in equimolar portions, or metathesis of **C**, $\mathbf{CH}^+Cl^-$, and Li·TCNQ, also

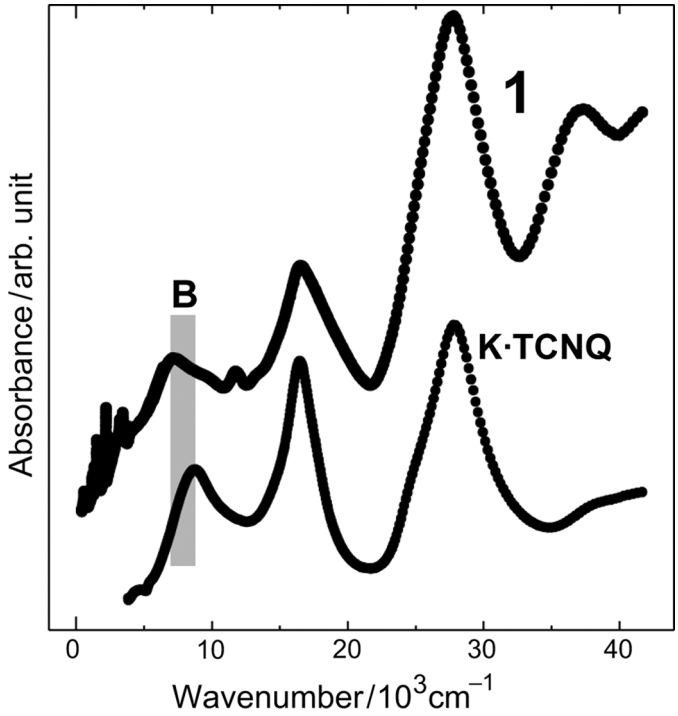

FIGURE 1 UV-vis-NIR spectra of **1** and K·TCNQ in KBr pellets. As for the assignment of Band-B, see the text.

produced **1**. Selected physical data of **1**: mp 211–214°C (dec). IR (KBr) 3400–2600, 2187, 2170, 2157, 1898, 1727, 1698, 1651, 1632, 1570, 1508 cm^{-1}. UV (KBr) 268, 362, 608, 850, 1410 nm. Anal. calcd. for $(C_4H_5N_3O)(C_4H_6N_3O)(C_{12}H_4N_4)$: C, 56.20; H, 3.54; N, 32.77; O, 7.49. Found: C, 56.30; H, 3.77; N, 32.64; O, 7.74.

Figure 1 compares the UV-vis-NIR spectra of **1** and K·TCNQ. Among the several absorption bands, a band at $8.5 \times 10^3\,cm^{-1}$ (labeled band B) in K·TCNQ is a characteristic of an electronic transition within the segregated column of a fully ionic $TCNQ^{\bullet-}$ [10]. The transition energy is related to the effective on-site Coulomb energy needed to transfer an electron from a certain $TCNQ^{\bullet-}$ site to another site in a fully anionic column. At less than $30 \times 10^3\,cm^{-1}$, **1** has a similar feature to K·TCNQ, except for a slight red shift of band B ($7.1 \times 10^3\,cm^{-1}$), confirming that the TCNQ molecule is ionized to $TCNQ^{\bullet-}$ in **1**. Because **1** did not exhibit an absorption band at less than $5 \times 10^{-3}\,cm^{-1}$, as seen in the partial CT state [11], the CT degree (γ) of TCNQ molecule in **1** is estimated to be 1. In agreement with this

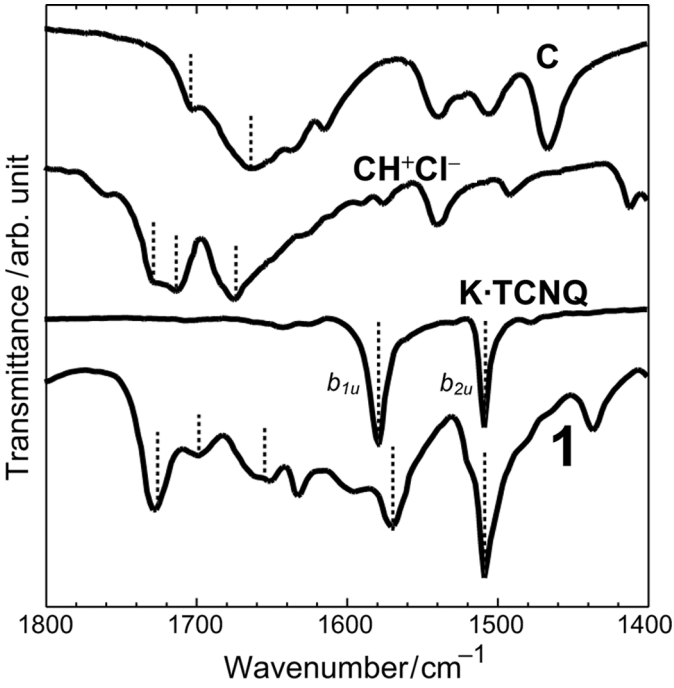

FIGURE 2 IR spectra of **1**, K·TCNQ, **C**, and $\mathbf{CH}^{+}\mathrm{Cl}^{-}$ in KBr pellets in the range of 1400–1800 cm^{-1}. Dashed lines indicate C=C and C=O stretching modes.

estimation, the C=C stretching modes in the IR spectrum (Fig. 2) of TCNQ (b_{1u}, b_{2u}), which are sensitive to molecular ionization while insensitive to short atomic contacts around TCNQ [11a], are similar to those of K·TCNQ. Whereas the C≡N stretching modes, which were conventionally used to estimate ionicity [12b], are very sensitive to atomic contacts around the C≡N groups (*vide infra*) and hence did not yield precise information on the ionicity of TCNQ in **1**.

The C=O stretching modes, which provide information on the **C** species of **1** (Fig. 2), are not simple superimposes of those of **C** and $\mathbf{CH}^{+}\mathrm{Cl}$, but peaks at 1727, 1698, and 1651 cm^{-1} are reminiscent of those in the cytidinium–cytidine pair [12]. Therefore, the **C** species in salt **1** is assigned to $\mathbf{CHC}^{+}$. Consequently, the optical data clearly deduced that **1** is represented as $(\mathbf{CHC})^{+}(\mathrm{TCNQ}^{\bullet -})$ with a segregated column of $\mathrm{TCNQ}^{\bullet -}$, consistent with both elemental analysis for the chemical formula and structural analysis for the chemical species and column structure.

Crystal Structure

Compound **1** crystallized in a triclinic system, and one **C** and half of TCNQ molecules are independent. No significant difference in the crystal structure was found between 200 and 9 K, and so the details are based on the data at 200 K. The ionicity of TCNQ was evaluated as approximately 1 based on the intramolecular bond lengths (Table 2) [13], which is in good agreement with the optical data. Uniform segregated stacks of $TCNQ^{\bullet -}$ columns were formed along the *a*-axis (Fig. 3), and a one-dimensional (1D) band structure was calculated by the tight-binding approximation based on the crystal structure. The interplanar distance between TCNQ molecules was 3.14 Å and decreased to 3.10 Å at 9 K, which was shorter than any other TCNQ salts with a uniform column (3.22–3.48 Å at RT), even taking the thermal contraction into account [14]. In sharp contrast to the 1D alkali metal $TCNQ^{\bullet -}$ salts exhibiting monomer–dimer transition above 200 K, due to spin-Peierls instability [15], the uniform TCNQ stacks in **1** could be preserved down to 9 K.

Two **C** molecules form a $\mathbf{CHC}^+$ pair by complementary triple HBs with two N3–H···O1 (2.84 Å) bonds and an N2–H···N2 bond (2.84 Å) (Fig. 4). Because the hydrogen atom on N2 is disordered into two sites with a site occupancy factor of 0.5, an inversion center is located at the center of $\mathbf{CHC}^+$. The $\mathbf{CHC}^+$ unit in **1** is symmetric, similar to those observed in ($\mathbf{CHC}^+$)[trichloroacetate] [7a], but different from the asymmetric $\mathbf{CHC}^+$ unit observed in ($\mathbf{CHC}^+$)[resorcylate]·H_2O, ($\mathbf{CHC}^+$)$_2$[$ZnCl_4$], [Ni(nta)(H_2O)$_2$]($\mathbf{CHC}^+$)·2H_2O (nta: nitrilotriacetic acid), and ($\mathbf{CHC}^+$)[BF_4] [7b–e]. Between $\mathbf{CHC}^+$ pairs, complementary double HBs (N3···O1 = 2.88 Å) exist, forming an infinite flat ribbon (//*b*, Fig. 5). Such a ribbon structure has been observed in [Ni(nta)(H_2O)$_2$]($\mathbf{CHC}^+$)·2H_2O [7d] and cytosine-5-acetic acid [8a]. In addition,

TABLE 2 Intramolecular C–C Bond Lengths of TCNQ Molecule in **1**, $TCNQ^0$ and Ionic $TCNQ^{\bullet -}$

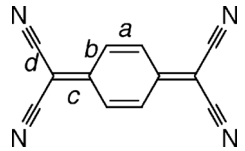

TCNQ Molecule	*a*/Å	*b*/Å	*c*/Å	*d*/Å
1	1.371(4)	1.413(4), 1.423(4)	1.416(4)	1.409(4), 1.420(4)
$TCNQ^0$[12a]	1.346	1.448	1.374	1.441
$TCNQ^{\bullet -}$[12b]	1.373	1.426	1.420	1.416

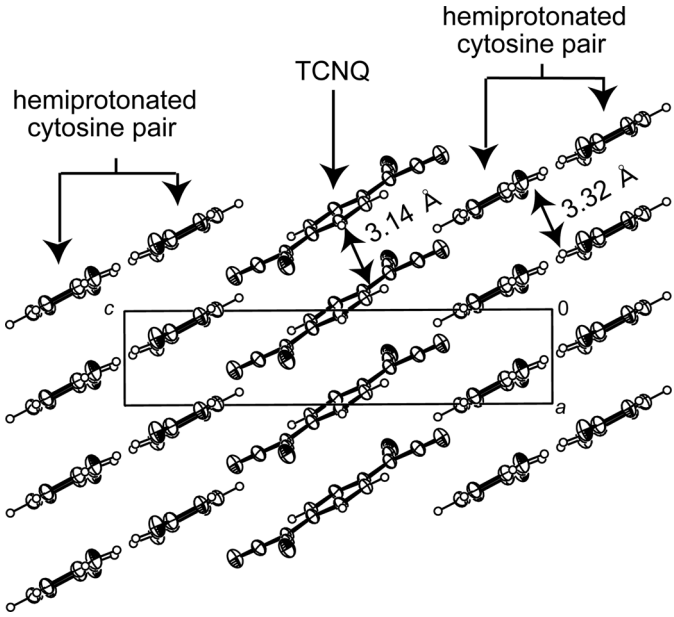

FIGURE 3 Crystal packing of **1** viewed along the *b*-axis at 200 K.

the $\mathbf{CHC}^+$ pair formed HBs with TCNQ (N1−H···N≡C, 2.88 Å) to establish a two-dimensional (2D) HB sheet (Fig. 5).

$\mathbf{CHC}^+$ ribbons stacked uniformly along the *a*-axis with an interplanar distance of 3.32 Å to form a thin polycationic layer in the *a*–*b* plane. In addition, a polyanionic layer was formed in the *a*–*b* plane by a weak C−H···N≡C HB (3.36 Å) connecting neighboring TCNQ columns. Therefore, the crystal is regarded as a layered compound consisting of an alternating arrangement of polycationic (9.10 Å wide) and polyanionic layers (8.23 Å) along the *c*-axis with robust HBs between them. These robust HBs stabilize the uniform layered structure even at low temperatures.

Electric and Magnetic Properties

It is known that fully ionic TCNQ radical salts with uniform stacks are insulators of Mott type with $\sigma_{RT} = 10^{-4}$–10^{-6} S cm^{-1} [15]. The electrical conductivity of **1** along the stacking direction at RT was 3×10^{-2} S cm^{-1} with an energy gap of 0.28 eV (Fig. 6). Such a large σ_{RT} value is because of the favorable uniform stacking of $TCNQ^{\bullet -}$ with a ring-over-bond type pattern and the short face-to-face distance in the TCNQ column. The temperature dependence of electrical

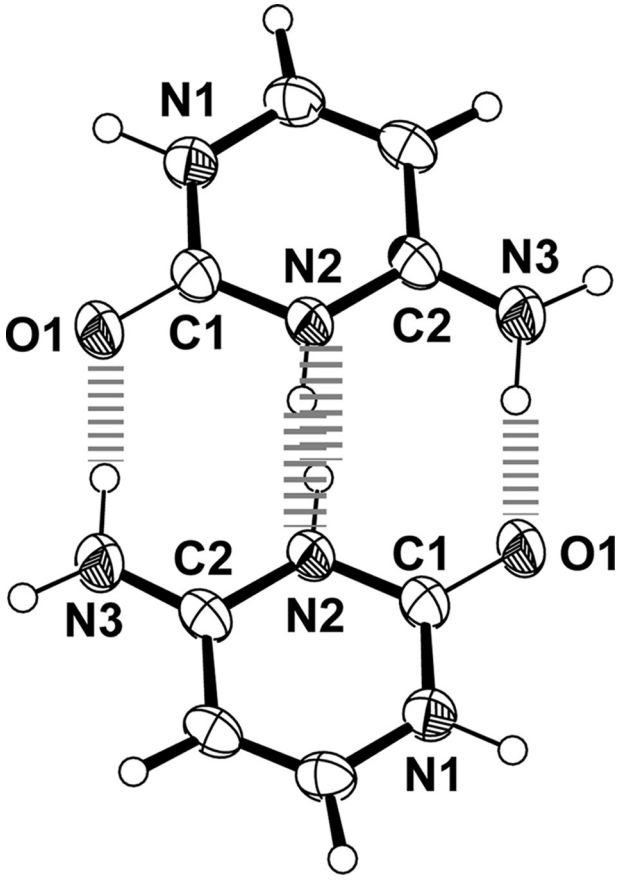

FIGURE 4 A $\mathbf{CHC}^+$ pair with complementary triple HBs.

conductivity between RT and 100 K showed no anomaly due to spin-Peierls transition, which is in agreement with the crystal structural analysis. The magnetic susceptibility value (χ_{stat}, 4.5×10^{-5} emu mol^{-1}) of **1** at RT indicates that only 3.6% of spins survive because of the considerable magnetic coupling by strong antiferromagnetic exchange (Fig. 7). No magnetic ordering such as spin-Peierls transition or antiferromagnetic ordering was present down to low temperatures (9 K), contrary to other conventional 1D $TCNQ^{\bullet -}$ Mott systems [15].

Stabilization of Uniform One-Dimensional Structure

To study the stabilization mechanism of the preservation of the uniform arrangement in the TCNQ column, we studied the self-asembling

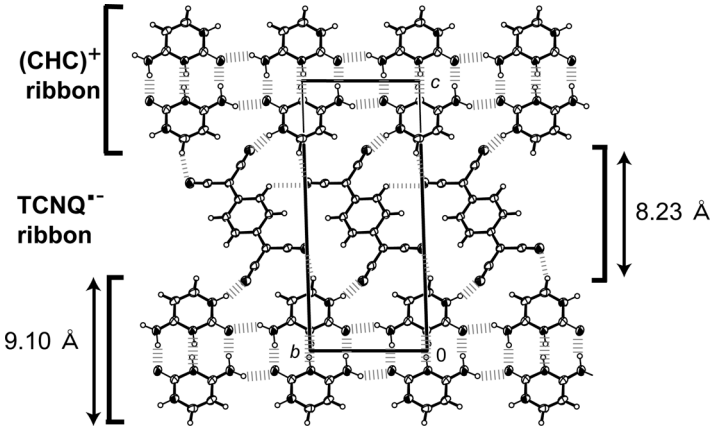

FIGURE 5 The *a*-axis projection of HB sheet of **CHC**$^+$ and TCNQ$^{\bullet-}$. Thick and thin dotted lines represent strong N–H···X (X = O, N) and weak C–H···N HBs, respectively.

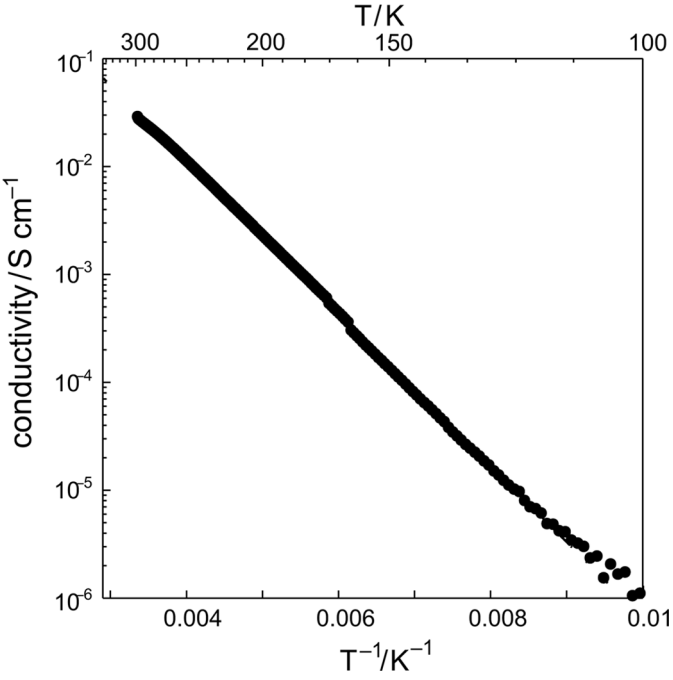

FIGURE 6 Temperature dependence of electric conductivity for a single crystal of **1** (//*a*).

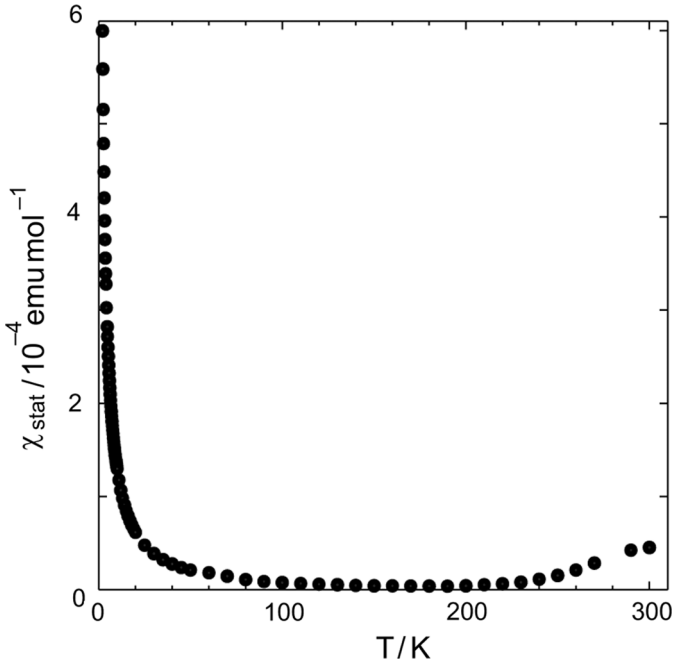

FIGURE 7 Temperature dependence of paramagnetic susceptibility for the polycrystalline sample of **1**.

natutre of $\mathbf{CHC}^+$ units. The theoretical calculation at the MP2/6-31G level [16] evaluated the stablization energy of the $\mathbf{CHC}^+$ assembly in **1** as -45 kcal mol^{-1} for the HB direction and as -16 kcal mol^{-1} for the π-stacking direction. They were larger than the dimerization energy of $TCNQ^{\bullet-}$ molecules (-10.4 kcal mol^{-1}) [17], and the monomer–dimer transition in the TCNQ column requires a large lattice energy to overcome the stabilization energy of $\mathbf{CHC}^+$ units. Therefore, the origin of the suppression of spin-Peierls transition in **1** is understood as the strong self-assembling nature of $\mathbf{CHC}^+$ units to form a one-dimensional ribbon along the side-by-side direction, robust HBs between **C** and TCNQ molecules, and π-stacking structure.

CONCLUSION

In summary, we have investigated the **C** incorporated CT solid, ($\mathbf{CHC}^+$)($TCNQ^{\bullet-}$) **1**, which established a new motif of crystal architecture constructed by complementary HBs in symmetric $\mathbf{CHC}^+$ ribbon, robust HBs between $\mathbf{CHC}^+$ and $TCNQ^{\bullet-}$ ribbons, and weak HBs

between $TCNQ^{\bullet -}$ columns. The HB interactions in **1** regulated the molecular arrangement to form a layered architecture and maintain a uniform stacking pattern. Furthermore, the robustness of complementary HBs and π-stacking structure inherent in the nucleobase system suppressed the spin-Peierls transition in **1**. These effects demonstrated a high conductivity of 3×10^{-2} S cm^{-1} for a fully ionic TCNQ salt. Our observations indicate that self-assembled architectures in biological systems would provide a promising strategy for the design of new molecular conductors. Furthermore, investigations are being conducted into the CT solids of other nucleobases and acceptors to demonstrate biomolecule-incorporated molecular conductors.

ACKNOWLEDGMENTS

This work was supported in part by a Grant-in-Aid (21st Century COE programs on Kyoto University Alliance for Chemistry and No. 15205019) from the Ministry of Education, Culture, Sports, Science, and Technology, Japan. T. M. is a recipient of research fellowships from the Japan Society for the Promotion of Science (JSPS).

REFERENCES

[1] (a) Slifkin, M. A. (1971). *Charge Transfer Interactions of Biomolecules*, Academic Press: London; (b) Eley, D. D. (1989). *Mol. Cryst. Liq. Cryst.*, *171*, 1.

[2] (a) Kasumov, A. Y., Kociak, M., Guéron, S., Reulet, B., Volkov, V. T., Klinov, D. V., & Bouchiat, H. (2001). *Science*, *291*, 280; (b) Zhang, Y., Austin, R. H., Kraeft, J., Cox, E. C., & Ong, N. P. (2002). *Phys. Rev. Lett.*, *89*, 198102.

[3] (a) Neilands, O. (2001). *Mol. Cryst. Liq. Cryst.*, *355*, 331; (b) Balodis, K., Khasanov, S., Chong, C., Maesato, M., Yamochi, H., Saito, G., & Neilands, O. (2003). *Synth. Met.*, *133–134*, 353; (c) Morita, Y., Maki, S., Ohmoto, M., Kitagawa, H., Okubo, T., Mitani, T., & Nakasuji, K. (2002). *Org. Lett.*, *4*, 2185; (d) Morita, Y., Miyazaki, E., Umemoto, Y., Fukui, K., & Nakasuji, K. (2006). *J. Org. Chem.*, *71*, 5631.

[4] (a) Slifkin, M. A. & Kushelevsky, A. P. (1971). *Spectrochim. Acta, Part A*, *27*, 1999; (b) Bazhina, I. N., Verzilov, V. S., Grechishkin, V. S., Grechishkina, R. V., & Gusarov, V. M. (1973). *Zh. Struct. Khim.*, *14*, 930; (c) Sheina, G. G., Radchenko, E. D., Blagoi, I. P., & Verkin, B. I. (1978). *Dokl. Akad. Nauk SSSR*, *240*, 463.

[5] Saito, G. & Yoshida, Y. *Bull. Chem. Soc. Jpn.*, award article, accepted.

[6] Dawson, R. M. C., Elliott, D. C., Elliott, W. H., & Jones, K. M. (Eds.) (1986). *Data for Biochemical Research*, 3rd ed. Clarendon Press: Oxford.

[7] (a) Gdaniec, M., Brycki, B., & Szafran, M. (1988). *J. Chem. Soc., Perkin Trans. II*, 1775; (b) Tamura, C., Sato, S., & Hata, T. (1973). *Bull. Chem. Soc. Jpn.*, *46*, 2388; (c) Fujinami, F., Ogawa, K., Arakawa, Y., Shirotake, S., Fujii, S., & Tomita, K. (1979). *Acta Crystallogr., Sect. B*, *35*, 968; (d) Salam, M. A. & Aoki, K. (2000). *Inorg. Chim. Acta*, *311*, 15; (e) Armentano, D., De Munno, G., & Rossi, R. (2006). *New J. Chem. 30*, 13.

[8] (a) Marsh, R. E., Bierstedt, R., & Eichhorn, E. L. (1962). *Acta Crystallogr.*, *15*, 310. (b) Gehring, K., Leroy, J.-L., & Guéron, M. (1993). *Nature*, *363*, 561; (c) Müller, J. & Freisinger, E. (2005). *Acta Crystallogr., Sect. E*, *61*, o320.
[9] Sheldrick, G. M. (1997). *Program for Crystal Structure Analysis*, University of Goettingen: Germany.
[10] Torrance, J. B. (1979). *Acc. Chem. Res.*, *12*, 79.
[11] (a) Meneghetti, M. & Pecile, C. (1986). *J. Chem. Phys.*, *84*, 4149; (b) Chappell, J. S., Bloch, A. N., Bryden, W. A., Maxfield, M., Poehler, T. O., & Cowan, D. O. (1981). *J. Am. Chem. Soc.*, *103*, 2442. It should be noted, however, that the authors of this paper used both b_{1u} and a_g modes of C≡N stretching in their analysis. If one uses only b_{1u} modes of IR spectra, the linear relation between $\upsilon_{C\equiv N}$ and the degree of CT (γ) is held only below $\gamma = 0.5$.
[12] Borah, B. & Wood, J. L. (1976). *J. Mol. Struct.*, *30*, 13.
[13] (a) Flandrois, P. S. & Chasseau, D. (1977). *Acta Crystallogr., Sect. B*, *33*, 2744; (b) Kistenmacher, T. J., Emge, T. J., Bloch, A. N., & Cowan, D. O. (1982). *Acta Crystallogr., Sect. B*, *38*, 1193.
[14] (a) Konno, M. & Saito, Y. (1974). *Acta Crystallogr., Sect. B*, *30*, 1294; (b) Konno, M. & Saito, Y. (1975). *Acta Crystallogr., Sect. B*, *31*, 2007; (c) Konno, M., Ishii, T., & Saito, Y. (1977). *Acta Crystallogr., Sect. B*, *33*, 763; (d) Kobayashi, H. (1981). *Bull. Chem. Soc. Jpn.*, *54*, 3669; (e) Kobayashi, H. (1978). *Acta Crystallogr., Sect. B*, *34*, 2818.
[15] (a) Hibma, T. & Kommandeur, J. (1975). *Phys. Rev. B*, *12*, 2608; (b) Kommandeur, J. (1980). In: *The Physics and Chemistry of Low Dimensional Solids*, Alcacer, L. (Ed.), D. Reidel: Dordrecht, Holland, 197; (c) Kommandeur, J. (1980). *NATO Advanced Study Institute Series, Series C*, *56*, 197.
[16] Šponer, J., Leszczynski, J., Vetterl, V., & Horba, P. (1996). *J. Biomol. Struct. Dyn.*, *13*, 695.
[17] Boyd, R. H. & Phillps, W. D. (1965). *J. Chem. Phys.*, *43*, 2927.